

# Pushing the Boundaries of Photovoltaic Light to Electricity Conversion: A GaAs Based Photonic Power Converter with 68.9% Efficiency

Henning Helmers, Esther Lopez\*, Oliver Höhn, David Lackner, Jonas Schön, Meike Schauerte, Michael Schachtner, Frank Dimroth, Andreas W. Bett

Fraunhofer Institute for Solar Energy Systems ISE, 79110 Freiburg, Germany

\*) now with: Instituto de Energía Solar, Universidad Politécnica de Madrid, Madrid, Spain

**Abstract**—We present recent results achieved in the field of photonic power conversion, i.e. monochromatic light to electricity conversion, using photovoltaic cells. Based on a thin film processing approach we leverage photon recycling and optical resonance effects with a GaAs/AlGaAs rear-heterojunction photovoltaic cell. A back reflector yields increased effective minority carrier lifetime and, as a consequence, an increase in voltage. Optical resonance in the microcavity yields high absorptance close to bandgap despite weak absorptivity. Hence, high current is reached while thermalization losses are minimized. Maximal spectral response  $SR=0.653$  A/W is measured at 858 nm. At this wavelength, thermalization losses diminish to only 21 meV per photon or 1.5%<sub>rel</sub>. Based on the calibrated spectral response combined with light  $I$ - $V$  measurements under broad band and monochromatic light, we determine a maximum equivalent monochromatic power conversion efficiency at 858 nm of 68.9%±2.8%.

**Keywords**—*photonic power converter, power-by-light, optical power transmission, photon recycling, resonance, microcavity, back reflector, thin film*

## I. INTRODUCTION

Besides solar power conversion, photovoltaic (PV) cells can also be used to convert artificial light into electricity. This is used in power-by-light systems, where light – often generated with lasers or light emitting diodes (LEDs) – is used to transmit power across distance, either through free space (wireless power transmission, laser power beaming) or through optical fiber (power-over-fiber). This technology receives increasing interest for various applications due to its advantage in comparison with traditional power transmission technologies of inherent galvanic isolation, and as a result avoidance of electromagnetic interferences, the possibility of actual wireless power transmission, and prospects of an elegant combination with optical data transmission.

PV cells in this application are also known as photonic power converters (PPCs). Due to the narrow band nature of the irradiance, PPCs can achieve higher power conversion

efficiency than solar cells under broad band solar illumination. This is because the two dominating loss mechanisms in solar cells, namely transmission and thermalization, can both be effectively suppressed.

In this work we report our recent achievement of a demonstration of unprecedented photovoltaic power conversion efficiency under monochromatic 858 nm light [1].

## II. METHODS

### A. Device structure and fabrication

We grew a GaAs/Al<sub>0.30</sub>Ga<sub>0.70</sub>As rear-heterojunction PV cell on a GaAs substrate using metal organic vapor phase epitaxy (MOVPE). Below the active PV cell layers a GaInP etch stop layer is introduced to allow for substrate removal.

The front side of the wafer is processed using standard fabrication steps including front side metallization, anti-reflective coating, and mesa etching. After the front side processing is finished, the wafer is flipped and bonded to a temporary handling substrate. Then, the substrate is removed by selective wet chemical etching. The now exposed rear side contact layer is structured using wet etching into a hexagonal pattern for subsequent point contacting. The remainder is coated with a back surface reflector. Here, two variations were investigated, namely a gold (Au) reflector and a dielectric-metal (MgF<sub>2</sub>/AlO<sub>x</sub>/Ag) reflector. Then, a low ohmic contact metallization is evaporated to contact and interconnect the rear side points. Afterwards, the rear side is reinforced with electroplated copper for mechanical stabilization. At last, the stabilized thin film wafer is debonded from the handling wafer. As a reference also a similar cell processed on GaAs substrate was fabricated. Figure 1 illustrates the process flow of the fabrication scheme, including a photography of the thin film wafer.

Further details about the epitaxial structure and the semiconductor processing can be found in [1].

### B. Calibrated spectral response

The relative spectral response  $SR_{rel}$  of the specimen was measured using a grating monochromator setup with adjustable bias voltage and bias spectrum on a temperature controlled chuck ( $T=25^\circ\text{C}$ ). For most of the wavelength range the

---

The work was partly funded by the German Federal Ministry of Education and Research (BMBF) through the project "Lightbridge" (16ES0788). E. L. acknowledges an Atracción del Talento Fellowship (2019-T2/AMB-12959) funded by the Comunidad de Madrid.

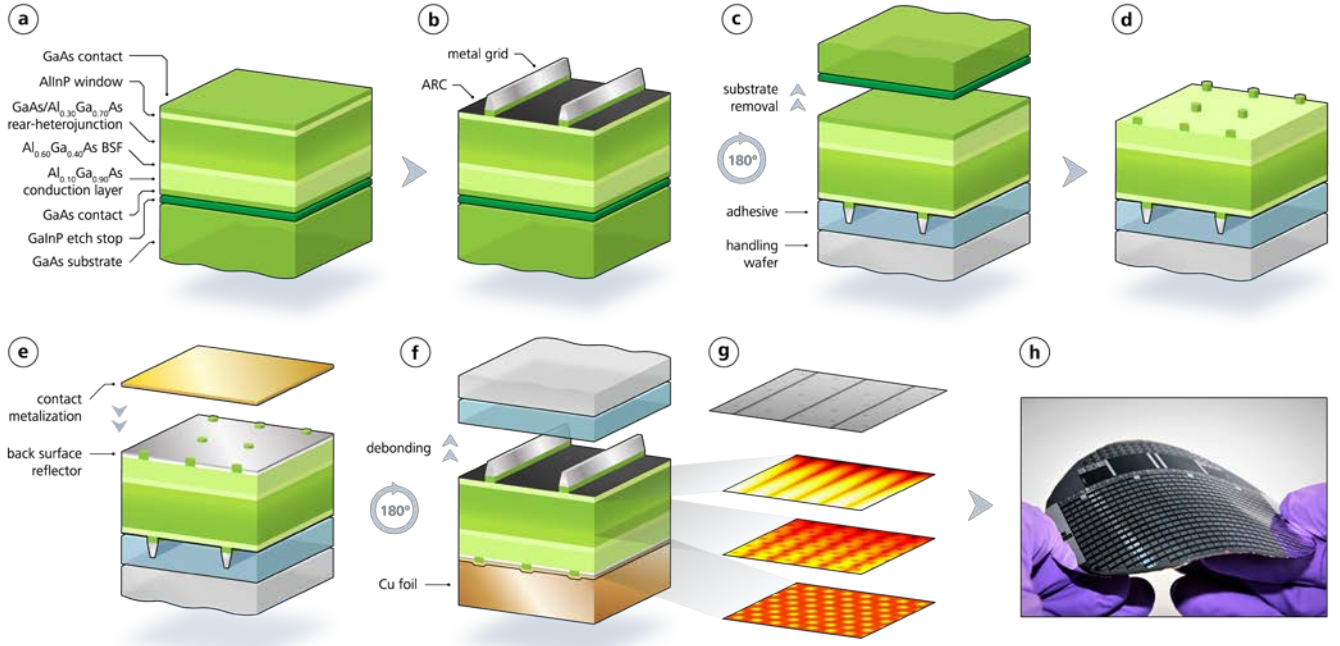


Fig. 1. Illustration of the fabrication steps to realize the thin film PPCs with back surface reflector. (a) Epitaxial layer structure of the n-GaAs/p-AlGaAs rear-heterojunction device. (b) Front side processing: Grid metallization and anti-reflection coating (ARC). (c) Transfer to handling wafer and substrate removal. (d) Hexagonal point contact pattern on the rear side. (e) Deposition of the structured back surface reflector and rear side contact metallization. (f) Cu electroplating to provide mechanical stabilization and debonding from handling wafer. (g) Top: Infrared micrograph of a PPC with Au back surface reflector and local point contacts under forward bias ( $V=1180$  mV,  $J_{mp}=0.44$  A/cm<sup>2</sup>). The front metal grid lines prevent electroluminescence emission from underneath leading to dark line features in the image. The rear point contacts are visible as darker circles as there is no reflector underneath. Bottom: The lower three images illustrate the lateral voltage drop at the front and rear side due to metal front grid lines and rear point contacts, respectively, and at the junction influenced by both features. The lower three images are obtained from electrical network modeling and show a different image section than the micrograph above. (h) Photograph of a flexible 4'' wafer after thin film processing with back surface reflector on copper foil. | Figure reproduced from [1] – Open access article under Creative Commons Attribution License.

measurement was conducted in the standard configuration of 10 nm steps. To increase the accuracy in vicinity of the bandgap, in the range 780 nm to 890 nm the resolution was increased by decreasing the entrance and exit slit widths of the grating monochromator (monochromatic light with 3 nm full width at half maximum) and the measurement was conducted in 2 nm steps. The actual designated area  $A$  was determined using an optical microscope. One-sun  $I$ - $V$  characteristics were measured on a temperature controlled chuck ( $T=25^\circ\text{C}$ ) under a spectrally adjustable sun simulator to generate the same short-circuit current  $I_{SC}$  as under illumination with the AM1.5d (ASTM G173-03) spectrum  $E(\lambda)$  ( $\int E d\lambda = 1000$  W/m<sup>2</sup>). The spectral irradiance of the sun simulator was determined with a spectroradiometer which was calibrated using a standard lamp. The intensity of the sun simulator was determined with a reference solar cell. Both standard lamp and reference solar cell were calibrated at the Physikalisch-Technische Bundesanstalt, the National Metrology Institute of Germany, traceable to national standards and, thus, to the international system of units (SI). The calibrated absolute spectral response  $SR$  was then determined as follows:

$$SR = \frac{I_{SC}/A}{\int SR_{rel} E d\lambda} SR_{rel} \quad (1)$$

### C. Equivalent monochromatic efficiency

For a PV cell with a linear dependence of its photo generated current, or more specifically of its spectral response  $SR(\lambda)$ , on

irradiance, we can use the short-circuit current  $I_{SC}$  of a light  $I$ - $V$  measurement under arbitrary illumination spectrum to calculate the corresponding equivalent monochromatic input power  $P_{in,\lambda}$  as follows:

$$P_{in,\lambda} = I_{SC} SR(\lambda) \quad (2)$$

With  $P_{mp}$  being the measured maximum output power determined from the  $I$ - $V$  curve, the equivalent monochromatic efficiency  $\eta_\lambda$  can, thus, be determined from measured quantities as follows [2]:

$$\eta_\lambda = \frac{P_{mp}}{P_{in,\lambda}} = \frac{P_{mp} SR(\lambda)}{I_{SC}} \quad (3)$$

This quantity  $\eta_\lambda$  is sometimes also called the spectral efficiency of a PV cell [3, 4] and can also be expressed using the derived quantity fill factor  $FF = P_{mp}/(I_{SC}V_{OC})$ :

$$\eta_\lambda = SR(\lambda) V_{OC} FF \quad (4)$$

It should be emphasized that this equivalent efficiency approach is only valid for devices where the device response is linear with irradiance and where the current collection probability and spectral response do not depend on the minority carrier generation profile in the absorber. This restriction usually holds for decently passivated materials and sufficient diffusion lengths. However, this approach is not valid e.g. for devices with

lower absorber material quality and neither for multi-junction cells. For the latter, the device current often strongly depends on the generation profile due to the series connection of subcells; and, in addition, luminescence coupling between the junctions often causes a non-linear response [5, 6].

### III. RESULTS & DISCUSSION

Figure 2 shows the spectral reflectance (symbols, right axis) of the investigated specimen. For the two thin film cells with back reflector, the reflectance steeply increases after the absorber becomes transparent at photon energies below the bandgap. Furthermore, a typical interference pattern is observed. Maximal reflectance reaches up to of 95.5% and is achieved

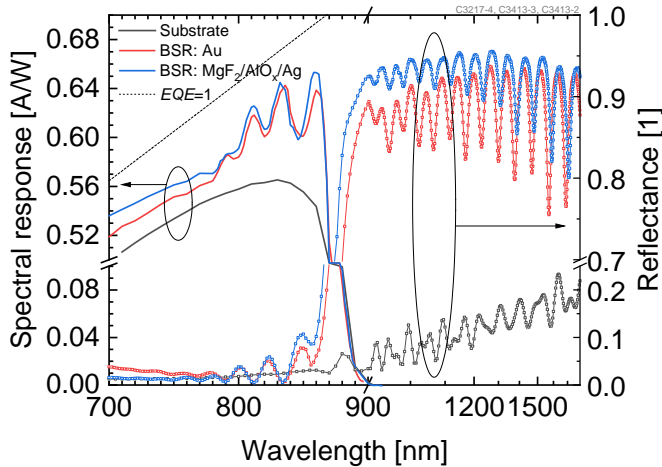


Fig. 2. Calibrated spectral response  $SR$  at  $T=25^\circ\text{C}$  and spectral reflectance  $R$  of the cells with back surface reflector (BSR) in comparison with a similar cell on substrate. The dashed line represents an  $EQE$  of unity. | Figure reproduced from [1] – Open access article under Creative Commons Attribution License.

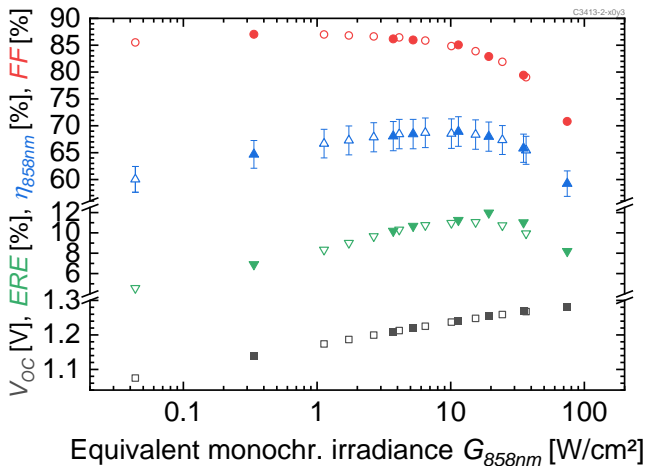


Fig. 3. Open-circuit voltage  $V_{OC}$ , experimental external radiative efficiency  $ERE$ , equivalent monochromatic efficiency at 858 nm  $\eta_{858nm}$ , and fill factor  $FF$  from light  $I$ - $V$  measurements as a function of equivalent monochromatic irradiance at 858 nm  $G_{858nm}$ . Open symbols represent data derived from measurements under broad band illumination, namely under a calibrated one-sun broad band light source (lowest current and irradiance, respectively) and using a Xenon flash bulb (rest). Solid symbols show data from  $I$ - $V$  curves recorded under a pulsed 809 nm laser; more details on the laser setup can be found in [7]. | Figure reproduced from [1] – Open access article under Creative Commons Attribution License.

with the dielectric-metal mirror. The lines corresponding with the left axis in Figure 2 show the calibrated spectral responses. The cells with back reflector show an increase in  $SR$  compared with the reference on substrate for all wavelengths, which can be attributed to the prolonged optical thickness due to the reflector. In vicinity of the bandgap, where absorptivity becomes weak, for the reference cell on substrate the  $SR$  drops due to limited absorptance. In contrast, for the thin film cells with back reflector a fringe pattern is observed indicating Fabry-Perot resonances in the microcavity. A maximal  $SR(858\text{ nm})=0.653\text{ A/W}$  is reached with the device with dielectric-metal reflector, which corresponds to an external quantum efficiency of  $EQE(858\text{ nm})=94.4\%$ . At this wavelength the difference between photon energy and bandgap energy of the absorber, which determines thermalization losses, is only 21 mV or 1.5%<sub>rel.</sub>

Figure 3 shows measured  $I$ - $V$  parameters  $FF$  and  $V_{OC}$  as well as the external radiative efficiency  $ERE$  and the equivalent monochromatic efficiency  $\eta_{858nm}$ , plotted as a function of equivalent monochromatic irradiance  $G_{858nm} = P_{in,858nm}/A$ . At low irradiances the latter increases as a result of the logarithmic increase in voltage with increasing irradiance. At high irradiances efficiency drops due to increasing series resistance losses scaling with current squared. At  $G_{858nm} = 11.4\text{ W/cm}^2$  the efficiency peaks at a record value of  $\eta_\lambda = 68.9\% \pm 2.8\%$ .

### IV. CONCLUSION

By implementing a back surface reflector to a thin film photovoltaic cell based on a high quality GaAs/AlGaAs rear-heterojunction, we introduce an optical cavity to leverage optical resonance to increase near bandgap absorptance as well as boost the output voltage due to photon recycling. The equivalent monochromatic power conversion efficiency was introduced, which can be derived from standard solar cell measurements under some constraints regarding the device and requiring knowledge of the spectral response in absolute units. It allows to determine efficiencies of photonic power converters without the need to perform measurements under laser light. Best performance was achieved with a thin film cell with a MgF<sub>2</sub>/AlO<sub>x</sub>/Ag reflector. We demonstrated an optical-to-electrical photovoltaic power conversion efficiency of  $68.9\% \pm 2.8\%$  for operation under monochromatic irradiance of  $11.4\text{ W/cm}^2$  at 858 nm. Highly efficient photonic power converters are a key ingredient to enable new and emerging applications of optical power transmission in various domains.

### ACKNOWLEDGMENT

The authors gratefully thank all “III-V” colleagues at Fraunhofer ISE for support with epitaxial growth, semiconductor processing, device characterization, and many valuable discussions.

### REFERENCES

- [1] H. Helmers, E. Lopez, O. Höhn, D. Lackner, J. Schön, M. Schauerer, M. Schachtner, F. Dimroth, A. W. Bett, “68.9% efficient GaAs based photonic power conversion enabled by photon recycling and optical resonance,” Phys. Status Solidi RRL, 2021. <https://doi.org/10.1002/pssr.202100113>
- [2] A. W. Bett, F. Dimroth, R. Löckenhoff, E. Oliva, J. Schubert, “III-V solar cells under monochromatic illumination,” in: Conf. Rec. 33<sup>rd</sup> IEEE

- Photovoltaic Specialists Conference (PVSC), 2008. <https://doi.org/10.1109/PVSC.2008.4922910>
- [3] M. A. Hamdy, F. Luttmann, D. Osborn, "Model of a spectrally selective decoupled photovoltaic/thermal concentrating system," *Appl. Energy*, vol. 30(3), pp. 209-225, 1988. [https://doi.org/10.1016/0306-2619\(88\)90046-3](https://doi.org/10.1016/0306-2619(88)90046-3)
- [4] Z. Yu, M. Leilaoui, Z. Holman, "Selecting tandem partners for silicon solar cells," *Nat. Energy*, vol. 1, 16137, 2016. <https://doi.org/10.1038/nenergy.2016.137>
- [5] M. Wilkins, C. E. Valdivia, A. M. Gabr, D. Masson, S. Fafard, K. Hinzer, "Luminescent coupling in planar opto-electronic devices," *J. Appl. Phys.*, vol. 118, 143102, 2015. <https://doi.org/10.1063/1.4932660>
- [6] E. Lopez, O. Höhn, M. Schuerte, D. Lackner, M. Schachtner, S. K. Reichmuth, H. Helmers, "Experimental coupling process efficiency and benefits of back surface reflectors in photovoltaic multi-junction photonic power converters," *Prog. Photovolt. Res. Appl.*, vol 29, pp. 461-470, 2021. <https://doi.org/10.1002/pip.3391>
- [7] S. K. Reichmuth, H. Helmers, C. E. Garza, D. Vahle, M. de Boer, L. Stevens, M. Mundus, A. W. Bett, G. Siefert, "Transient I-V Measurement Set-Up for Photovoltaic Laser Power Converters under Monochromatic Irradiance," in: *Proc 32<sup>nd</sup> European Photovoltaic Solar Energy Conference and Exhibition (EU PVSEC)*, pp. 5-10, 2016. <https://doi.org/10.4229/EUPVSEC20162016-1AO.1.2>